

BRAIN COMMUNICATIONS

Principal component analysis, a useful tool to study cyclin-dependent kinase-inhibitor's effect on cerebral ischaemia

Lucas Le Roy,¹ Ahmed Amara,¹ Cloé Le Roux,¹ Ozvan Bocher,¹ Anne Létondor,¹ Nathalie Benz¹ and Serge Timsit^{1,2}

Stroke is a leading cause of acute death related in part to brain oedema, blood–brain barrier disruption and glial inflammation. A cyclin-dependant kinase inhibitor, (S)-roscovitine, was administered 90 min after onset on a model of rat focal cerebral ischaemia. Brain swelling and Evans Blue tissue extravasation were quantified after Evans Blue injection. Combined tissue Evans Blue fluorescence and immunofluorescence of endothelial cells (RECA1), microglia (isolectin-IB4) and astrocytes (glial fibrillary acidic protein) were analysed. Using a Student's *t*-test or Mann–Whitney test, (S)-roscovitine improved recovery by more than 50% compared to vehicle (Mann–Whitney, $P < 0.001$), decreased significantly brain swelling by 50% (*t*-test, $P = 0.0128$) mostly in the rostral part of the brain. Main analysis was therefore performed on rostral cut for immunofluorescence to maximize biological observations (cut B). Evans Blue fluorescence decreased in (S)-roscovitine group compared to vehicle (60%, *t*-test, $P = 0.049$) and was further supported by spectrophotometer analysis (Mann–Whitney, $P = 0.0002$) and Evans Blue macroscopic photonic analysis (*t*-test, $P = 0.07$). An increase of RECA-1 intensity was observed in the ischaemic hemisphere compared to non-ischaemic hemisphere. Further study showed, in the ischaemic hemisphere that (S)-roscovitine treated group compared to vehicle, showed a decrease of: (i) endothelial RECA-1 intensity of about 20% globally, mainly located in the cortex (-28.5% , *t*-test, $P = 0.03$); (ii) Microglia's number by 55% (*t*-test, $P = 0.006$) and modulated reactive astrocytes through a trend toward less astrocytes number (15%, *t*-test, $P = 0.05$) and astrogliosis (21%, *t*-test, $P = 0.076$). To decipher the complex relationship of these components, we analysed the six biological quantitative variables of our study by principal component analysis from immunofluorescence studies of the same animals. Principal component analysis differentiated treated from non-treated animals on dimension 1 with negative values in the treated animals, and positive values in the non-treated animals. Interestingly, stroke recovery presented a negative correlation with this dimension, while all other biological variables showed a positive correlation. Dimensions 1 and 2 allowed the identification of two groups of co-varying variables: endothelial cells, microglia number and Evans Blue with positive values on both dimensions, and astrocyte number, astrogliosis and brain swelling with negative values on dimension 2. This partition suggests different mechanisms. Correlation matrix analysis was concordant with principal component analysis results. Because of its pleiotropic complex action on different elements of the NeuroVascular Unit response, (S)-roscovitine may represent an effective treatment against oedema in stroke.

- 1 Univ Brest, Inserm, EFS, UMR 1078, Genetics, functional genomics and biotechnology (GGB), F-29200, Brest, France
- 2 Neurology and Stroke Unit Department, CHRU de Brest, Université de Bretagne Occidentale, Inserm 1078, France

Correspondence to: Prof. Serge Timsit, Faculté de Médecine et des Sciences de la Santé, 22 avenue Camille Desmoulins, 29238 Brest Cedex 3, France
E-mail: serge.timsit@chu-brest.fr

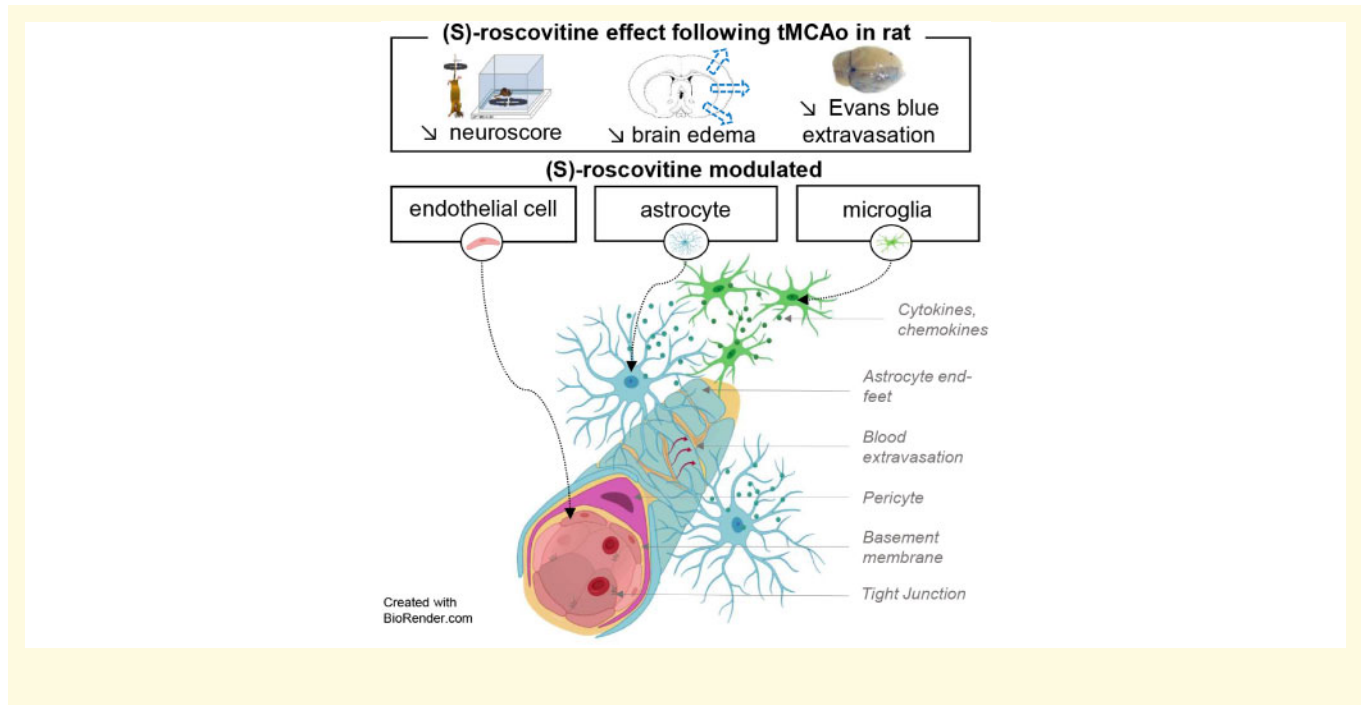
Keywords: ischaemic stroke; CDK inhibitor; oedema; NeuroVascular Unit

Received April 20, 2020. Revised June 30, 2020. Accepted July 6, 2020. Advance Access publication August 31, 2020

© The Author(s) (2020). Published by Oxford University Press on behalf of the Guarantors of Brain.

This is an Open Access article distributed under the terms of the Creative Commons Attribution Non-Commercial License (<http://creativecommons.org/licenses/by-nc/4.0/>), which permits non-commercial re-use, distribution, and reproduction in any medium, provided the original work is properly cited. For commercial re-use, please contact journals.permissions@oup.com

Abbreviations: BBB = blood–brain barrier; CDK = cyclin-dependent kinases; DGN = deep grey nuclei; EB = Evans Blue; GFAP = glial fibrillary acidic protein; IB4 = isolectin-IB4; IBA-1 = ionized calcium-binding adapter molecule 1; MCA = middle cerebral artery; MW = Mann–Whitney; NVU = NeuroVascular Unit; OCT = optimal cutting temperature; PCA = principal component analysis; RECA1 = Rat Endothelial Antigen 1; ROI = regions of interest; tMCAo = transient middle cerebral artery occlusion.



Introduction

In 2016, the number of stroke-related deaths was 5.5 million, the number of disability-adjusted life-years (DALYs) lost was 116 million, there were 13.7 million new strokes cases (Johnson *et al.*, 2019). Life-threatening, space-occupying brain oedema occurs in 1–10% of patients with acute supratentorial infarct (Shaw *et al.*, 1959; Frank, 1995; Sakai *et al.*, 1998). The prognosis of malignant middle cerebral artery (MCA) infarctions is poor, with case fatality rates of nearly 80% (Hacke *et al.*, 1996; Berrouschot *et al.*, 1998). No medical treatment has been proven effective. In patients with malignant MCA infarction, decompressive surgery undertaken within 48 h of stroke onset reduces mortality and increases the number of patients with a favourable functional outcome and is the only approach that showed its efficacy (Vahedi *et al.*, 2007; Hofmeijer *et al.*, 2009).

Oedema has two components: cytotoxic and vasogenic oedema (Michinaga and Koyama, 2015). Cytotoxic oedema is a massive cell swelling affecting mainly astrocytes, caused by anion and cation intracellular accumulation, due in part to failure of ATP-dependent Na^+/K^+ pumps. Vasogenic oedema, due to blood–brain barrier (BBB) disruption, induces extravasation of plasma, serum proteins and water. Ischaemic cascade and blood flow restoration contribute to Neurovascular Unit (NVU)

inflammation which causes BBB permeability increase. The BBB permeability allows the infiltration of leukocytes involved in oedema formation and in inflammatory cytokines release that promotes inflammation of brain parenchyma.

Roscovitine is a potent inhibitor of cyclin-dependent kinases (CDK) 1, 2, 5, 7 and 9 and exists in two stereoisomers, (R)- and (S)-roscovitine (Meijer *et al.*, 1997; Bach *et al.*, 2005). CDKs are a family of kinases first known for their role of cell cycle regulators but also involved in a different process. In particular, CDK5 is implicated in multiple cellular processes in the central nervous system including neuronal migration and synaptic signalling (Ohshima *et al.*, 1999; Li *et al.*, 2001). Increasingly, *in vitro* and *in vivo* evidences show the role of CDKs and, CDK5 hyperactivation in neuronal death during ischaemic stroke (Love, 2003; Wen *et al.*, 2005; Meyer *et al.*, 2014; Shin *et al.*, 2019). (S)-roscovitine showed a neuroprotective effect *in vitro* and in two experimental murine models of focal cerebral ischaemia (Menn *et al.*, 2010; Rousselet *et al.*, 2018).

Studies on transient middle cerebral artery occlusion (tMCAo) rat model showed that (S)-roscovitine was able to dramatically decrease brain oedema (Rousselet *et al.*, 2018). Here, we investigate the mechanisms implicated in the anti-oedematous effect of (S)-roscovitine in tMCAo rat 48 h after reperfusion (Fig. 1A), we hypothesized that

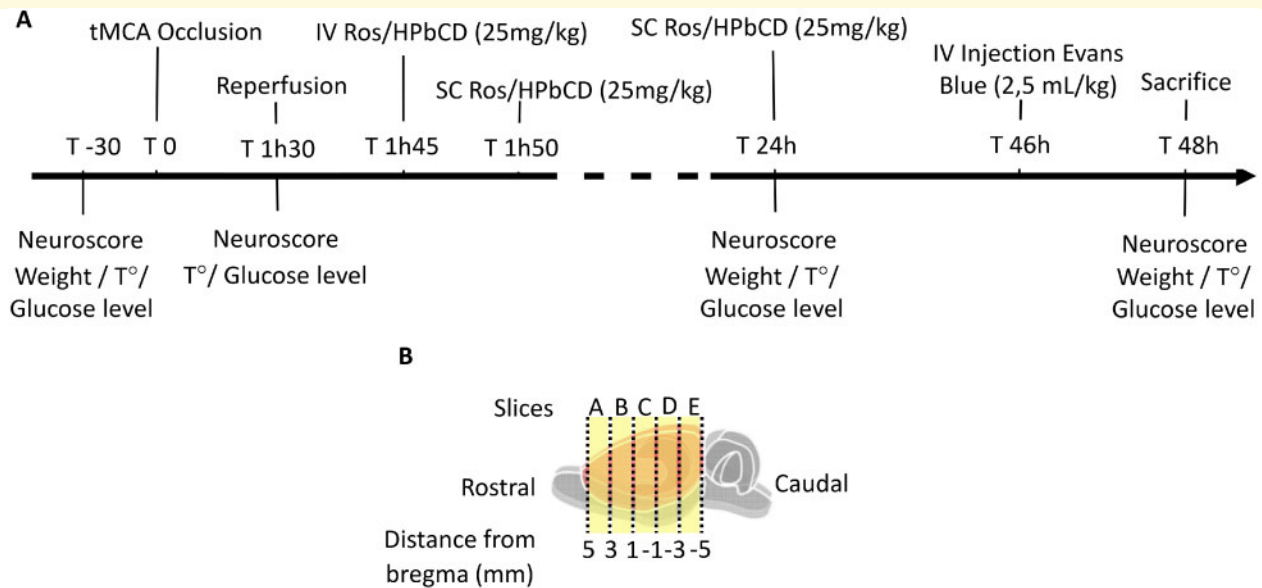


Fig. 1 Experimental design. Transient focal cerebral ischaemia was induced in adult Sprague-Dawley rats by transient occlusion of middle cerebral artery for 90 min (A). (S)-roscovitine ($n = 15$) or its vehicle (cyclodextrin) ($n = 16$) was administered 15 min post-reperfusion by an intravenous bolus (25 mg/kg body weight) followed by subcutaneous injection (25 mg/kg body weight) 20 min post-reperfusion and 24 h post-reperfusion. Neurological scoring was performed before surgery, just prior to reperfusion, 24 h post-tMCAo and 48 h post-tMCAo. EB was injected through lateral tail vein (2.5 ml/kg) 46 h post-tMCAo and then animals were euthanized and brain was removed and cut in 5 coronal slices A, B, C, D, E (B).

(S)-roscovitine effect may be mediated by a complex modulation of the NVU. To test our hypothesis, we designed an NVU integrated approach to study (S)-roscovitine effect on oedema, BBB disruption, endothelial cells, astrocytes and microglia.

Materials and methods

Animals

Adult male Sprague-Dawley rats (360–500 g bodyweight) were purchased from Janvier Labs (Le Genest-Saint-Isle, France) and housed in pairs. All rats were kept in a temperature-controlled room ($21 \pm 0.5^\circ\text{C}$) under a 12-h light/dark cycle. All experiments were conducted in accordance with directives from the European Community Council (2010/63/EU) and French legislation (code rural et de la pêche maritime, in particular articles R.214-87 to R.214-126) on animal experimentation. Procedures were validated by the Animal Experimentation Ethics Committee No. 074 and the MINISTÈRE DE L'ENSEIGNEMENT SUPERIEUR, DE LA RECHERCHE, ET DE INNOVATION under the number APAFIS#12925-2018010511189374 and are reported in compliance with the ARRIVE (Animal Research: Reporting In Vivo Experiments) guidelines (Kilkenny *et al.*, 2010) and the principles of replacement, refinement and reduction (3Rs). A previous study made it possible to refine the doses of inhibitor used on the animal, and thus to reduce the

number of animals used (Rousselet *et al.*, 2018). In order to limit the stress and the pain of the animals, an acclimatization period of 1 week will be respected on their arrival. They were housed collectively, in an enriched environment with a Polyvinyl chloride tunnel. Forty-two animals were included in this study, 31 in the first experiment set and 11 in the second experiment set. All rats had ad libitum access to food and water.

Surgical procedure

tMCAo was achieved as previously described (Menn *et al.*, 2010; Rousselet *et al.*, 2018). Briefly, rats were deeply anaesthetized and maintained with 2% isoflurane in air. Rectal temperature was maintained at $37 \pm 0.5^\circ\text{C}$ with a heating pad. After temporary suture of the common and external carotid arteries and coagulation of the external carotid artery, a 4–0 monofilament suture (4037PK5Re, Doccol Corporation) was introduced into the right internal carotid artery lumen and advanced until resistance was felt (± 20 mm). After anaesthesia recovery, a neurological score was performed just before 90 min of ischaemia onset. Then animals were anaesthetized again for withdrawal of monofilament to allow MCA reperfusion. The temporary suture on the external carotid artery was permanently tied off to prevent blood loss, and the caudal temporary suture placed around the common carotid artery was removed to allow cerebral blood flow release. Finally, 15 min after reperfusion, an intravenous

jugular vein injection of 1.9 ml of vehicle solution (30% hydroxypropyl β -cyclodextrin in phosphate buffer) or (S)-roscovitine (25 mg/kg in vehicle solution) at a flow rate of 0.48 ml/min was performed. Cyclodextrin allowed the maximum solubilization of (S)-roscovitine among several excipients available for human injectable formulation (Menn *et al.*, 2010). The animals were sutured and two subcutaneous injection of 1.9 ml of the same solution were performed 5 min after intravenous and 24 h post-ischaemia (25 mg/kg). Post-operative care and observation were carried out until the animal recovered consciousness and included post-operative subcutaneous injection of saline solution, subcutaneous administration of buprenorphine (0.05 mg/kg) and provision of softened food and gelled water. The weight, blood glucose level and body temperature of the animals were measured 30 min before surgery, at the time of occlusion (0'), just before reperfusion, at 24 and at 48 h (Supplementary Table 1).

Exclusion criteria

The following exclusion criteria were used: (i) rats with combined neurological score < 2.5 just before reperfusion (T 1h15) were immediately excluded and euthanized; (ii) rats which had no Evans Blue (EB) extravasation visible in fresh slices; (iii) rats which had no infarct visible in triphenyl tetrazolium chloride staining; (iv) rats that died within 48 h; (vi) rats that reached the study's endpoint (Supplementary Table 2) were immediately excluded and euthanized (Supplementary Figure 1).

Quality control for data collection and data processing

Rats were allocated to treatment groups. All measurements were assessed under blind conditions (L.L.R.), and brain swelling and EB extravasation volume were performed by two independent researchers (L.L.R. and C.L.R.).

Neurological scoring procedure

Neurological function was assessed just prior to reperfusion, 24 h and 48 h post-surgery using the modified method of (Jiang *et al.*, 2005) consisting in summing of the results of two behavioural tests scored on a 0-to-4 scale each (Supplementary Table 3). To assess a potential beneficial effect of treatment on behavioural outcome, recovery level was calculated as follows.

$$\text{Recovery (\%)} = \left[\frac{\left(\frac{\text{Total neurological score T 1h30} - \text{Total neurological T 49h30}}{\text{Total neurological score T 1hT}} \right)}{\text{Total neurological score T 1hT}} \right] * 100.$$

Experimental procedures

Two independent set of experiments were carried out and described below. The first experiment set ($n = 31$) included EB studies and immunofluorescence analysis

[$n = 8$ vehicle; $n = 8$ (S)-roscovitine], and biochemical analysis for western blot [$n = 8$ for vehicle; $n = 7$ for (S)-roscovitine]. The second experiment set ($n = 11$) concerned microglia staining with ionized calcium-binding adapter molecule 1 (IBA1) marker to support our prior results [$n = 5$ for vehicle and $n = 6$ for (S)-roscovitine].

EB injection

Forty-six hours after tMCAo, 2.5 ml/kg of 4% EB diluted in NaCl was injected by the lateral tail vein. Animals were sacrificed 48 h after tMCAo by intraperitoneal injection of pentobarbital sodique. Then, 200 ml of prewarmed 0.9% saline (37°C) at an outflow of 18.5 ml/min was injected through the left cardiac ventricle for 15 min to wash EB away from the circulation. The brain was immediately removed from the skull and placed into a brain matrix. The olfactory bulb and cerebellum were dissected, and then the brain was cut in five 2 mm-coronal-slice. Whole brain and five coronal brain slices pictures were taken to measure the brain swelling. In slices A, C and E, right hemisphere (lesioned) of the brain was separated from the left along the mid-line, and both sides were immediately frozen in liquid nitrogen for spectrophotometer analysis. Slices B and D were fixed in 4% paraformaldehyde for 24 h followed by 48 h sucrose immersion and embedded in optimal cutting temperature compound for immunohistochemical analysis. Forty micrometre thick sections were cut using cryostat in the coronal plane from optimal cutting temperature embedded slices B and D.

Brain swelling and EB extravasation measurement

Ischaemic ipsilateral hemispheres (iH) and contralateral hemisphere (cH) volume were measured in coronal sections images using the ImageJ software in double-blinded condition. Brain swelling was then calculated as a percentage of the hemispheres volume according to the following formula:

$$\text{Brain swelling} = \left[\frac{(\text{Vol iH} - \text{Vol cH})}{\text{Vol cH}} \right] * 100.$$

EB extravasation volume was then calculated as a percentage of the iH volume according to the following formula:

$$\text{EB extrav. volume} = \frac{\text{Vol EB}}{\text{Vol iH}} * 100.$$

Spectrophotometer analysis

Each hemisphere slice was weighed and homogenized separately in 0.5 ml phosphate-buffered saline and 0.5 ml of trichloroacetic acid (100%). Brain samples were centrifuged for 20 min at 10 000 rpm and allowed to cool

down at 4°C for 10 min. For fluorescent measurement, an aliquot was diluted 1:3 with ethanol. Fluorescence of EB was measured at an excitation wavelength of 620 nm and an emission wavelength of 680 nm (Microplate reader Varioscan Flash). Calculations were based on external standards in the solvent (100 ng/ml–3.333 µg/ml).

Immunohistofluorescence analysis

B and D tissues slices were washed for 30 min in a phosphate-buffered saline solution containing 0.3% triton 100× to permeabilize cell membranes. Next, to block nonspecific binding, the tissue was saturated with a solution containing 5% Normal Goat Serum (abcam, ab7481) for 1 h. Tissues were incubated at 4°C with the microglia marker isolectin-IB4 (IB4; 1:100, Thermofisher Scientific I21411) during 48 h or rabbit glial fibrillary acidic protein (GFAP) antibody (1:200, Invitrogen 53989282) and mouse RECA-1 antibody (1:200, Biorad MCA970GA) overnight. IB4 and GFAP were directly conjugated with an Alexa 488 dye treatment. Slices incubated with RECA-1 were then incubated with an anti-mouse secondary antibody conjugated with Alexa488 (1:1000, Thermofisher Scientific A-11001). Slices were mounted in a medium with 4',6-diamidino-2-phenylindole (Fluoromount-G™). Observations were made using the Zeiss Axio Imager M2 microscope. For IB4 staining, cell count was performed at 20× magnification on three regions of interest (ROI) in the cortex and three in deep grey nuclei (DGN) for each slice. DGN ROI were mainly located in the putamen. RECA-1 intensity and GFAP cell intensity were measured on 20× magnification pictures on two ROI in the cortex and two ROI in DGN. The ROIs were located respectively in the cH, EB extravasation zone (Infarct), the area surrounding the infarct (perilesional) and the area immediately in contact with infarct (boundary). Results were expressed relative to healthy hemisphere ROI.

Immunohistology

Animals were sacrificed 48 h after tMCAo and perfused with saline at 37°C followed by 4% paraformaldehyde fixation through the left cardiac ventricle. The brain was immediately removed from the skull and placed in a brain matrix and the olfactory bulb and cerebellum were removed. Brain was fixed in 4% paraformaldehyde for 24 h and then paraffin embedded. Ten micrometre slices were cut on microtome. Immunohistochemical analysis was achieved on tissue with anti-IBA1 (1:400; Wako 019-19741) coupled with horseradish peroxidase and stained using diaminobenzidine. Slides were scanned by nanozoomer HAMAMATSU and Image analysis was performed with NIS-Elements program (Nikon). ROI were measured on the cortex of a healthy hemisphere, ischaemia boundary area and infarct core. ROI from infarct

core and boundary were combined to calculate ipsilateral area fraction.

Biochemical analysis

Animals were sacrificed 48 h after tMCAo as previously described. The olfactory bulb and cerebellum were removed, and a first 2 mm-coronal-slice was cut and triphenyl tetrazolium chloride stained to confirm ischaemia. The rest of iH and cH were snap-frozen separately. Whole hemispheres were then homogenized by tissue-lyser in radioimmunoprecipitation buffer (150 mM NaCl, 25 mM Tris-HCl Ph7.5, 1% Triton x100, 0.1% sodium dodecyl sulfate, 1% Na deoxycholate, 10 mM iodoacetamide and 100 µM phenylmethylsulfonyl fluoride), supplemented with protease inhibitor cocktail tablets (Complete tablets, ROCHE) in the ratio of 1 tablet/10 mL radioimmunoprecipitation buffer. After centrifugation at 14.5 g for 15 min at 4°C, the supernatant fluid was collected. The total protein concentration of each sample was determined using Lowry protein assay (Lowry *et al.*, 1951). Soluble fraction aliquots were frozen and stored until use at 80°C.

Western blot

Equivalent protein amounts from each sample were heated at 70°C for 10 min for denaturation, resolved by electrophoresis using a 10% sodium dodecyl sulfate–polyacrylamide gel and transferred to polyvinylidene fluoride membranes. Blots were blocked for 1 h at room temperature in blocking solution (Tris-buffered saline containing 0.1% Tween-20 and 5% non-fat dried milk). Blots were incubated overnight at 4°C with primary antibody anti-occludin (1:200, 711500 Invitrogen) diluted in blocking solution and for 2 h at room temperature with secondary antibody conjugated with horseradish peroxidase (1:10 000, 31460 Thermofisher). Specific immunoreactivity was visualized using chemiluminescence enhanced chemiluminescence and enhanced chemiluminescence imager. Molecular masses of detected products were estimated by their migratory proximity to prestained protein markers (Biorad, Mississauga, ON). Following their initial use, each blot was stripped and reprobed with anti-β-actin (1:20 000) to provide a control for load variations between samples. Image Studio™ Lite program was used to measure the density of bands on western blots in a blinded manner. The relative optical densities within a same area size were measured for each sample, and normalized to the relative optical densities obtained for its corresponding β-actin. The resulting (S)-roscovitine and vehicle values in ischaemic and healthy hemisphere were then compared using a non-paired, two-tailed Student's *t*-test. Significant differences were accepted to *P*-values <0.05. Each blot was duplicated to validate the results. Normalization of densitometric data to untreated control (assigned a value of 100) was used for data presentation

in order to factor out run-to-run variability between absolute densitometry values assigned to an individual slot.

Statistical analysis

Sample sizes were determined based on previous tMCAo studies with (S)-roscovitine performed in our laboratory (Rousselet *et al.*, 2018). The statistical comparison between treated and non-treated animals for the different quantitative variables studied was performed on the GraphPad Prism 5 software (San Diego, USA). Gaussian distribution of the variables was tested by the Shapiro–Wilk normality test. Gaussian variables were then analysed by a two-tailed unpaired Student's *t*-test, whereas non-Gaussian distributed variables were analysed by a non-parametric Mann–Whitney (MW) *U* test. For all the tests, the significance threshold was set at 0.05.

Principal component analysis and correlation matrix

Principal component analysis (PCA) was used to study the similarities between individuals based on six variables measured on slice B: brain swelling volume, BBB disruption (EB extravasation fluorescence intensity), endothelial cell activation (RECA 1 intensity), microglia and astrocyte number, and astrogliosis (GFAP intensity/cell). The stroke recovery level was also included as a supplementary quantitative variable, i.e., it was not used in the PCA computations, but it was displayed on the correlation plot to help to interpret the dimensions of variability. (S)-roscovitine treatment was also included as a categorical supplementary variable [binary variable with two categories: (S)-roscovitine versus vehicle to group individuals and construct confidence ellipses]. PCA computation and representation were conducted on the R software using the packages FactoMineR and FactoExtra. Prior to the analysis, all variables were standardized.

A correlation matrix was also computed to study the relationship between the seven variables using the package 'corrplot' in the R software.

Data availability

The data that support the findings of this study are available from the corresponding author, upon reasonable request.

Results

Baseline characteristics

Mortality and physiological parameters were recorded throughout the tMCAo procedure and until the day of sacrifice (Supplementary Table 1). Body temperature was maintained around 37°C throughout the anaesthesia procedure and did not show a significant difference before

or after reperfusion. On the day of sacrifice, no difference was observed between the vehicle group and the treated group concerning temperature and glucose concentration for experiment set 1 and 2.

(S)-roscovitine improved neurological score

Analysis of neurological score progression over time showed that (S)-roscovitine treated group presented a significantly lower neurological score, so a higher recovery level, than vehicle-treated group at 48 h (MW $P=0.001$) (Table 1, experiment # 1). Both suspension subscore and rotation subscore were significantly higher on vehicle-treated group than in (S)-roscovitine.

(S)-roscovitine decreased brain swelling

(S)-roscovitine treatment decreased brain swelling by about 50% 48 h after reperfusion cortex [(S)-roscovitine: $9.8 \pm 9.8\%$ versus vehicle: $20.6 \pm 6.7\%$; *t*-test $P=0.0128$] (Fig. 2C). The difference between (S)-roscovitine and vehicle-treated groups took place mostly in the rostral side of the brain (Slice A, B and C) (Fig. 2D).

(S)-roscovitine reduced EB extravasation

(S)-roscovitine group presented a trend toward a decreased EB extravasation, measured on macroscopic observations, by about 30% [(S)-roscovitine: $21.6 \pm 9.9\%$ versus vehicle: $31 \pm 12.9\%$; (*t*-test $p=0.07$)] (Fig. 2E). Similarly to oedema measurement, the difference between (S)-roscovitine and vehicle-treated groups took place principally in the rostral side of the brain [Slice A (9.3% versus 25.35% , *t*-test, $P=0.03$) and B ($19.8 \pm 34.4\%$, *t*-test, $P=0.049$)] (Fig. 2F). In addition, EB spectrophotometry measurement on slices A, C and E (Fig. 2G), showed on rostral slice A considerable decrease of EB extravasation on (S)-roscovitine treated group (iH/cH = 1.1 ± 0.22) compared to vehicle (3.73 ± 3.2) (MW, $P=0.0002$). No differences between groups were observed on more caudal slices C and E.

EB extravasation decrease after treatment was associated with endothelial RECA-I labelling decrease and preservation of dimeric occludin form

EB fluorescence analysis on rostral slices B (Fig. 3A–C) showed that (S)-roscovitine group presented a significantly lower level of EB (1.15 ± 0.19) than the vehicle group (1.74 ± 0.74) (*t*-test $P=0.049$) (Fig. 3C and D). An increase of RECA-1 intensity was observed on infarct zone

Table 1 Neuroprotective effect of (S)-roscovitine on neurological score

	T 1 h 30		T 48 h		Recovery 48 h (%)	
	Median (25%; 75%)	Range	Median (25%; 75%)	Range	Median (25%; 75%)	Range
Combined						
Vehicle (n = 16)	4 (3.12; 4.8)	(2.5–6)	5 (4.5; 6.5)	(3–8)	–21.59 (–45.83; –12.95)	(–180 to 10)
(S)-roscovitine (n = 15)	4.5 (4; 5)	(3–5)	3 (3; 4.5)**	(0–6.5)	33.33 (0; 40)**	(–62.5 to 100)
Tail suspension						
Vehicle (n = 16)	2 (1.5; 2)	(1–3)	2.5 (2; 3)	(1–4)	–22.5 (–87.5; 0)	(–250 to 0)
(S)-roscovitine (n = 15)	2 (2; 2.5)	(1.5–2.5)	2 (1.5; 2.5)*	(0–3.5)	20 (–25; 40)**	(–75 to 100)
Spontaneous rotation						
Vehicle (n = 16)	2.25 (2; 3)	(1–3.5)	3 (2.12; 3.5)	(2–4)	–20 (–50; 0)	(–150 - 33,3)
(S)-roscovitine (n = 15)	2.5 (2; 3)	(1–3.0)	1.5 (1; 2)***	(0–3.5)	40 (0; 60)**	(–75 - 100)

Rats underwent neurological scoring [vehicle: n = 16; (S)-roscovitine: n = 15] just prior reperfusion (T 1 h 30) and 48 h post-MCAo. Recovery was calculated as a percentage of neurological score decrease from 90 min. Data are presented as median and interquartile. Data were analysed by the MW test to compare behavioural deficit between the groups at each time.

* $P \leq 0.05$; ** $P \leq 0.01$ and *** $P \leq 0.001$.

(Cortex: $+81.6 \pm 67.1\%$; DGN: $+66.5 \pm 72.9\%$) and on perilesional region (Cortex: $+49.6 \pm 33.2\%$; DGN: $+31.5 \pm 19.3\%$) of the vehicle group compared to cH (Fig. 3E). No significant difference between vehicle and (S)-roscovitine groups on the infarct zone was observed. Normalized RECA-1 intensity comparison in the perilesional area showed a trend toward a decrease of endothelial RECA-1 intensity of about 20% globally in the treated group compared to vehicle ($+20 \pm 26\%$ versus $+40 \pm 37\%$; MW=0.11) mainly located in the cortex ($+21.1 \pm 22.4\%$ versus $+49.6 \pm 33.2\%$) (t -test, $P=0.03$). In addition, morphological observation at $63\times$ showed on vehicle group a more degraded cell staining, on perilesional and on infarct region than on cH (Fig. 3C). Western blot analysis of tight-junction protein occludin showed a decrease of the damaged monomeric form of the protein on (S)-roscovitine group compared to vehicle ($-17.5 \pm 24.6\%$; t -test $P=0.032$) (Fig. 3F). No variation between groups was measured on the contralateral non-ischaemic hemisphere. Full-size blots are provided as [Supplementary material \(Supplementary Fig. 2\)](#).

(S)-roscovitine decreased microglia's number

In the adjacent sections, number of IB4-positive microglia was measured (Fig. 4A and B). For microglia number, the comparison of treated versus non-treated: (S)-roscovitine group showed a significantly lower number of microglia per mm^2 ($108 \pm 70 \text{ cell}/\text{mm}^2$) than vehicle group ($240 \pm 107 \text{ cell}/\text{mm}^2$) (t -test $P=0.006$) (Fig. 4C). This decrease was observed both in cortex [(S)-roscovitine: $129 \text{ cell}/\text{mm}^2 \pm 68$ versus vehicle: $250 \text{ cell}/\text{mm}^2 \pm 129$, MW $P=0.0325$] and the DGN [(S)-roscovitine: $87 \text{ cell}/\text{mm}^2 \pm 80$ versus vehicle: $230 \text{ cell}/\text{mm}^2 \pm 95$; t -test $P=0.003$].

In addition, IBA1 staining experiments (Fig. 4D and E) showed that (S)-roscovitine treatment decreased by 41% microglia density in the ipsilateral ischaemic hemisphere compared to the vehicle (0.0211 ± 0.0098 versus 0.0358 ± 0.0165 ; t -test $P=0.050$).

(S)-roscovitine modulated reactive astrocytes

In order to quantify the effect of (S)-roscovitine on astrogliosis after cerebral ischaemia, GFAP immunolabelling was performed on adjacent sections (Fig. 5A–C). Analysis was performed on cH, EB extravasation periphery zone (Perilesional and Boundary) and EB extravasation zone associated with infarction. Quantification of astrocytes number showed that they were very few isolated astrocytes in the infarct area of vehicle and (S)-roscovitine groups. However, in the perilesional-boundary area, there was a trend toward a decrease of astrocytes number in the (S)-roscovitine group ($350 \text{ cells}/\text{mm}^2 \pm 99$) compared to vehicle ($422 \text{ cells}/\text{mm}^2 \pm 65$) (t -test $P=0.05$) (Fig. 5D). This decrease took place only in DGN in which astrocytes number was $337 \text{ cells}/\text{mm}^2 \pm 130$ in (S)-roscovitine group compared to $469 \text{ cells}/\text{mm}^2 \pm 96$ in the vehicle group (t -test $P=0.019$) but not in the cortex: (S)-roscovitine: 362 ± 88 versus vehicle: 375 ± 103 , t -test $P=0.39$.

(S)-roscovitine group presented a trend toward smaller normalized GFAP intensity per astrocyte ($168.1 \pm 54.95\%$) compared to vehicle group (213.6 ± 65.0) (t -test $P=0.076$). This trend took place mainly in the DGN [vehicle: $202.3 \pm 87.5\%$; (S)-roscovitine: $153.3 \pm 55.6\%$; t -test $P=0.10$] but was not confirmed in the cortex [vehicle: 218.0 ± 68.8 ; (S)-roscovitine: 182.9 ± 79.5 ; t -test $P=0.18$].

Joint analysis of the effect of (S)-roscovitine on the different variables

PCA was used to study the similarities between individuals based on six variables measured on slice B: brain swelling volume, EB fluorescence intensity, RECA 1 intensity, microglia and astrocyte number, and astrogliosis (GFAP intensity/cell). Stroke recovery level was projected as a supplementary quantitative variable. PCA

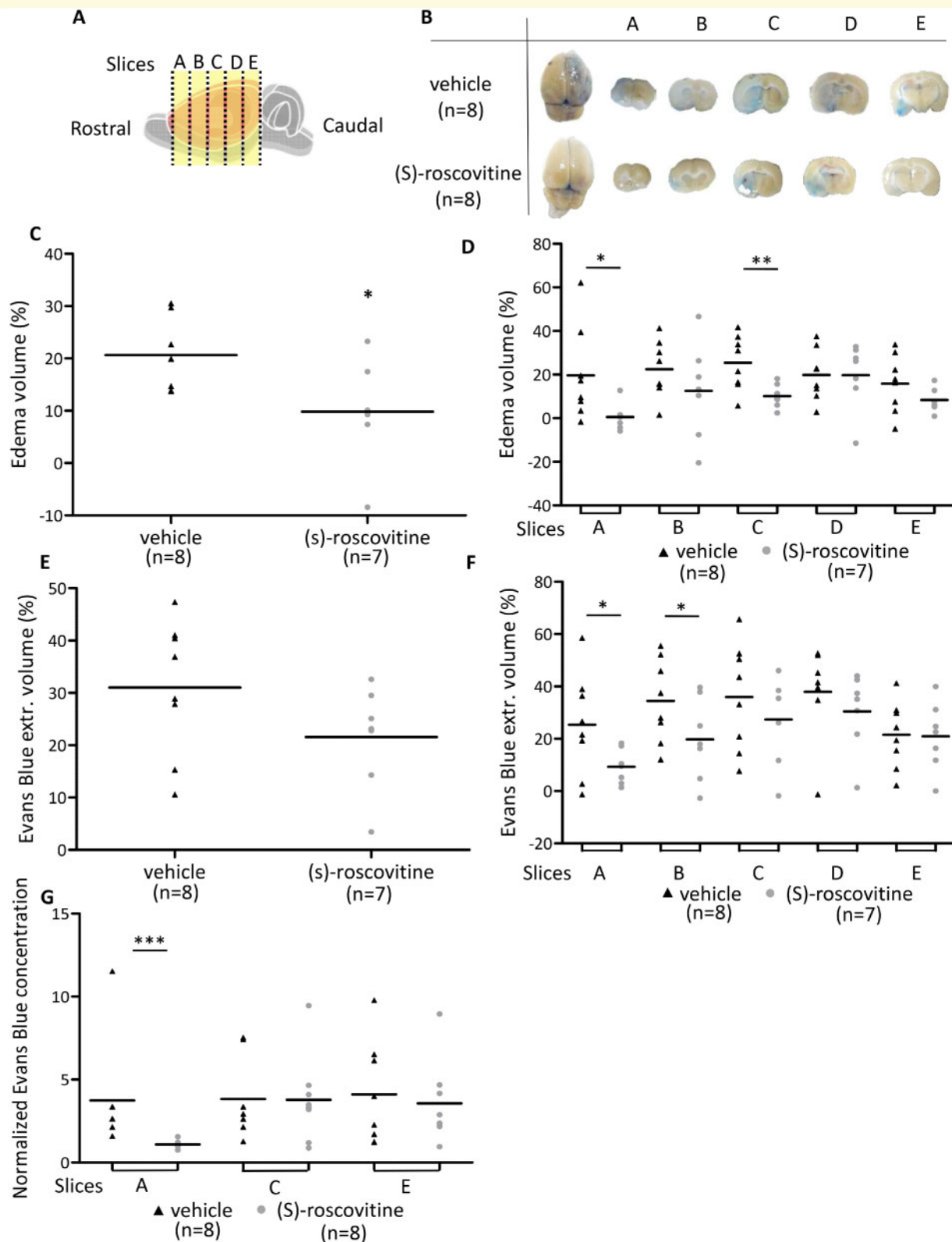


Fig. 2 (S)-roscovitine decreases brain swelling and EB extravasation after tMCAO. (A) Rostro-caudal slices A, B, C, D, E. Macroscopic pictures of the slices in (S)-roscovitine group ($n = 8$) and vehicle group ($n = 8$). (B) To calculate brain swelling volume (C), as the average of brain swelling volume of each slice (D). On these pictures, EB extravasation volume was also measured (E), as an average of EB extravasation volume of each slice (F). Spectrophotometric analysis of EB extravasation was carried out on slice A, C and E (G). Measurements were performed by two blind operators. * $P \leq 0.05$; ** $P \leq 0.01$; *** $P \leq 0.001$.

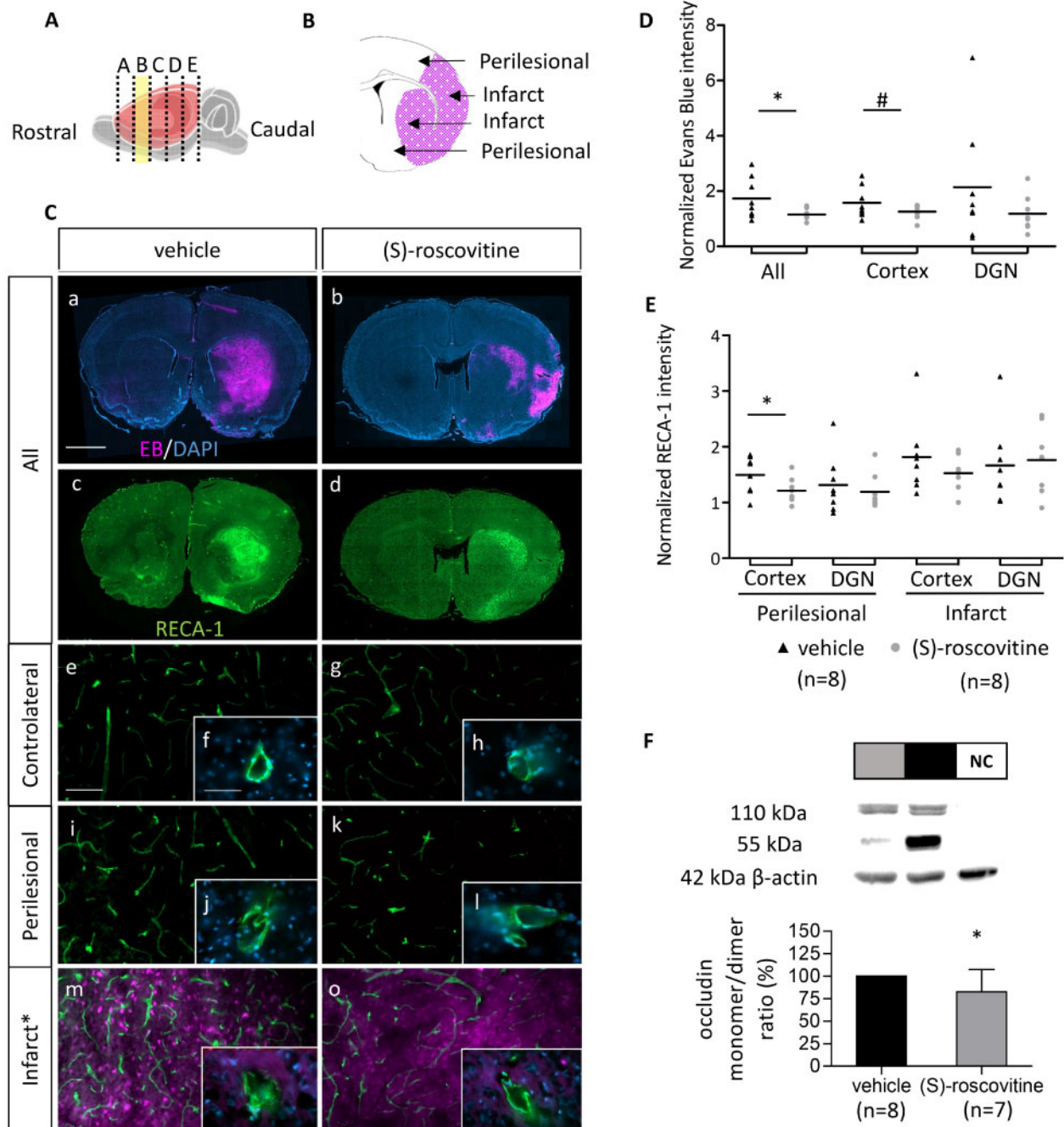


Fig. 3 EB extravasation decrease is associated with RECA-1 signal inhibition and preservation of dimeric occludin form.

(A) Rostro-caudal position of slice B, used for endothelial assessment. (B) Two analysed regions: cortex and DGN of ischaemic hemisphere called perilesional and infarct, respectively around and in the EB extravasation area (purple). EB emits at 680 nm, i.e., in red, however, to make the figures easier to interpret for colour blind readers, we converted red channel to purple (original red colour can be seen in [Supplementary Fig. 3](#)). (C) Immunohistochemical analysis of slice B of EB and endothelial cells on (S)-roscovitine ($n = 8$) and vehicle group ($n = 8$). EB extravasation fluorescence (a, b) was measured on the entire hemisphere, the cortex, and the DGN (D). Scale bars length is 2 mm. On the same section, endothelial cells were labelled with RECA-1 antibody (c, d). Intensity of RECA-1 was measured on Infarct and Perilesional region of cortex and DGN and normalized by contralateral RECA-1 intensity (E). Measurements were performed by blind operator. Morphological state of endothelial cell was observed on contralateral (e, f, g, h), perilesional (i, j, k, l) and infarct (m, n, o, p) regions of (S)-roscovitine and vehicle group at 20 \times (Scale bar length is 100 μ m) and 63 \times (Scale bar length is 50 μ m) magnification. Occludin concentration on the brain was measured on different animals treated with (S)-roscovitine ($n = 7$) or vehicle ($n = 8$) (F). Results are expressed as a ratio of monomer (55 kDa) and dimer conformation (110 kDa) of the protein, on ipsilateral ischaemic hemisphere. NC = negative control. Error bars expressed standard deviation. * $P < 0.05$; # $P < 0.10$.

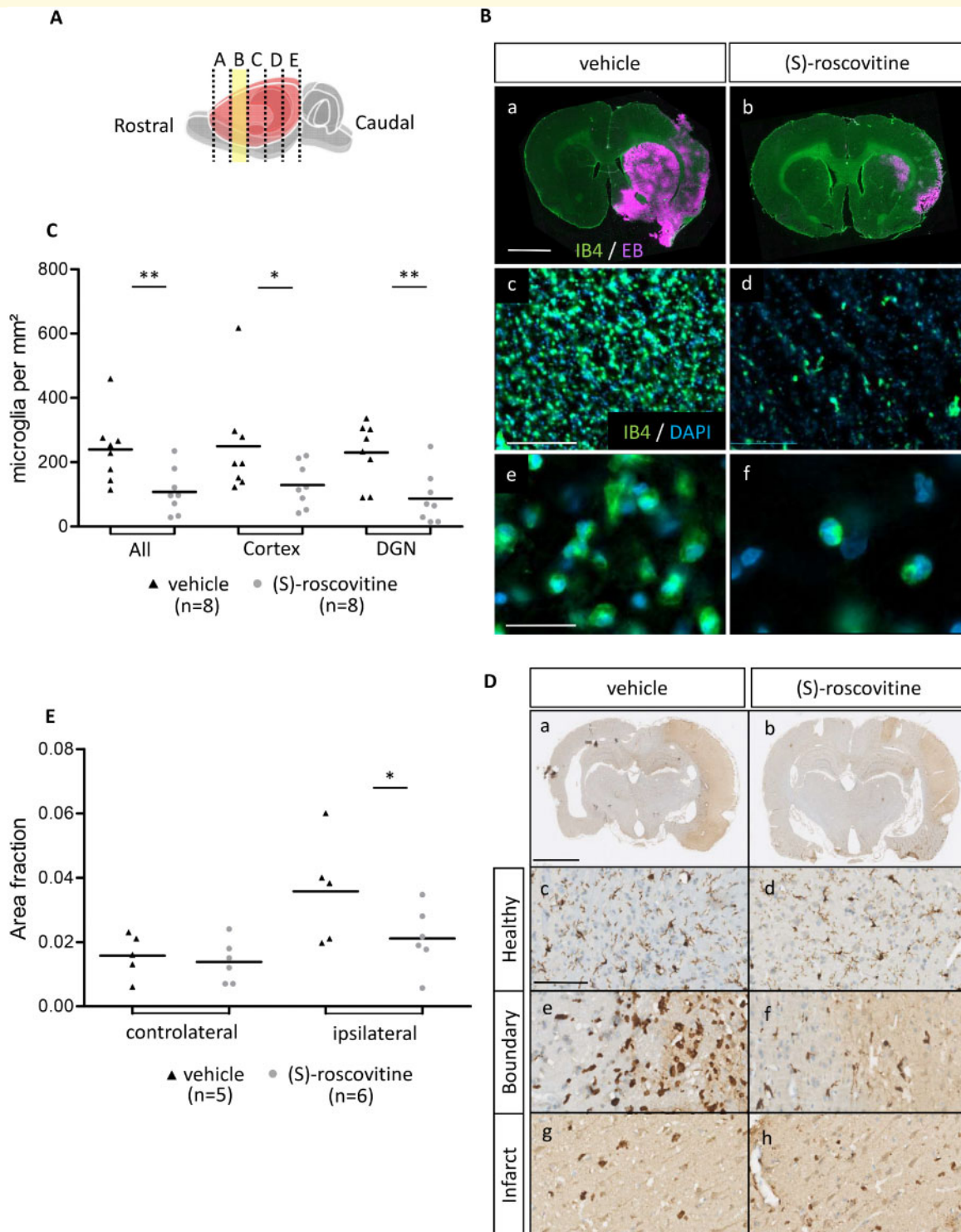


Fig. 4 (S)-roscovitine decreases microglia's number. (A) Rostro-caudal position of slices B, used for analysis. **(B)**

Immunohistochemical analysis on slice B of EB and microglia (a, b) in (S)-roscovitine ($n = 8$) and vehicle group ($n = 8$) (Scale bar length is 2 mm). Isolectin B4 marking was used for microglia count (c, d) (Scale bar length is 100 μm). Microglia were differentiated from blood vessels by morphological observation (e, f and [Supplementary Fig. 3](#)) (Scale bar length is 50 μm). Measurements were performed by blind operator. Number of microglia was measured on cortex and DGN and combined in total measurement **(C)**. **(D)** Immunohistochemical analysis of the second experimental protocol on paraffin-embedded tissue of (S)-roscovitine treated animal ($n = 6$) and vehicle-treated animal ($n = 5$). Microglia were labelled with IBA1 antibody coupled with horseradish peroxidase and stained by diaminobenzidine. Microglia density was measured on healthy cH (c, d), on boundary (e, f) and infarct (g, h) region of cortex. IBA1-positive area fraction in border and infarct were combined to calculate ipsilateral area fraction **(E)**. ROI were placed by blind operator and area fraction calculation was performed with NIS-Elements program (Nikon). a, b: Scale bars length is 2 mm; c–h: Scale bars length is 100 μm . * $P < 0.05$; ** $P < 0.01$.

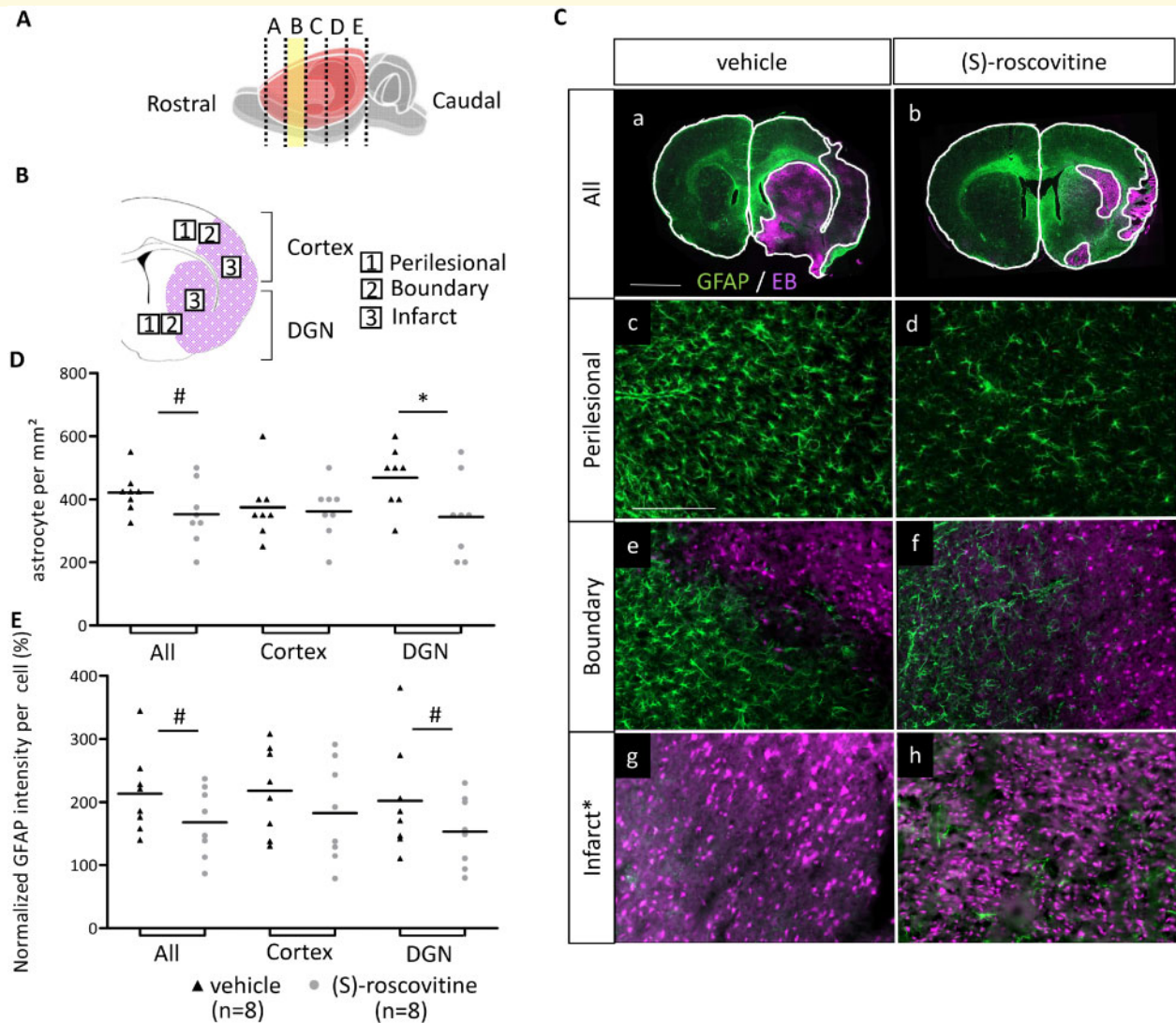


Fig. 5 (S)-roscovitine effect on astrocytes' number and astrogliosis. (A) Rostro-caudal position of slice B, used for analysis. (B) The three analysed regions in the cortex and DGN of ischaemic hemisphere called perilesional, boundary and infarct, respectively around the border and in the EB extravasation area (red). (C) Immunohistochemical analysis on slice B of EB and astrocytes (a, b) on (S)-roscovitine ($n=8$) and vehicle group ($n=8$) (Scale bars length is 2 mm). Astrocytes were labelled with GFAP antibody. Number of astrocytes and intensity of GFAP per astrocytes were measured on perilesional (c, d), boundary (e, f) and infarct (g, h), region of cortex and DGN (Scale bars length is 100 μ m). Measurements were performed by blind operator. Number of astrocytes in perilesional and border region were combined and represented in table (D). Intensity of GFAP per astrocytes in perilesional and border was normalized by contralateral GFAP intensity per astrocyte and combined in table (E). * $P \leq 0.05$; # $P \leq 0.10$.

differentiated (S)-roscovitine treated from non-treated animals (vehicle-treated) on dimension 1 (Fig. 6A) with the non-treated animals presenting positive values on dimension 1 and the (S)-roscovitine treated animals negative values. Treated animals seem to be globally more homogeneous than non-treated animals as shown by the size of the confidence ellipse around the barycentre of each group. All six cellular variables showed a positive correlation with dimension 1 (Fig. 6A). Among them, astrocyte's and microglia's numbers, brain swelling and EB were the ones with the highest values, and thus probably

the ones the most implicated in the discrimination of treated from non-treated animals. On dimension 2, RECA-1 and astrogliosis showed the highest correlation with opposite effects. Based on these two first principal component, it was possible to separate two groups of variables: the first group includes RECA-1, the number of microglia and EB that have positive values on both dimensions and the second group includes astrogliosis, astrocyte's number and brain swelling that show positive values on dimension 1, and negative ones on dimension 2 (Fig. 6A and B).

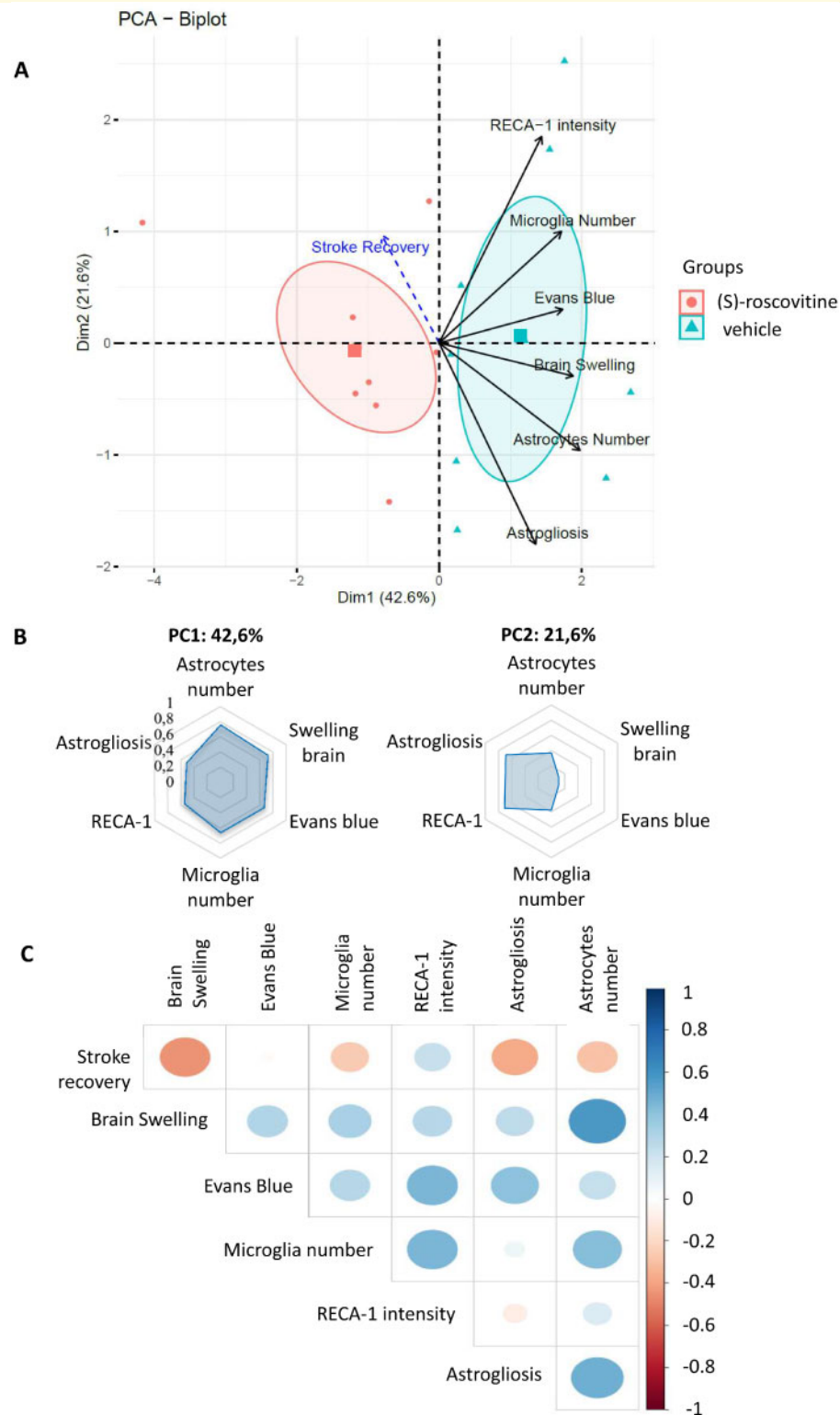


Fig. 6 PCA. PCA of six variables measured on 16 individuals [vehicle $n = 8$; (S)-roscovitine $n = 8$]: oedema volume, EB extravasation intensity, endothelial cells activation (RECA-1 intensity), microglia and astrocytes number (cell/mm²) and astrogliosis (GFAP intensity/cell) (**A**). Recovery was projected on the model. An individual who is on the same side of a given variable has a high value for that variable. An individual who is on the opposite side of a given variable has a low value for that variable. PCA biplot: variance explained by PCA biplot is 64.2% (principal component 1: 42.6%; PC2: 21.6%). Barycentres (square symbols) representing the centre of mass of individuals of each group of rats, and their corresponding 95% confidence ellipse were also added on the PCA representation (**B**). Correlation of variables with dimension 1 (principal component 1) and dimension 2 (PC2) (**C**). Correlation matrix of variables: positive correlations are displayed in blue and negative correlations in red colour. Colour intensity and the size of the circle are proportional to the correlation coefficients.

Correlation matrix, computed to study the relationship between the seven variables (Fig. 6C), showed that stroke recovery was highly negatively correlated with brain swelling and moderately negatively correlated with astrogliosis. On the opposite, positive correlations were observed between the astrocyte number and brain swelling, and, to a lesser extent, between microglia number and astrogliosis. Microglia number was moderately positively correlated with RECA-1 intensity and astrocytes number. Finally, EB was moderately positively correlated with RECA-1 and astrogliosis. These results are concordant with the ones obtained on the PCA analysis, where a positive correlation is found between the majority of the variables, except the stroke recovery which was the only one with negative values on the first dimension of the PCA. Furthermore, the majority of high positive correlations were observed between variables that were found to co-vary in the dimension 2 of the PCA.

Discussion

Our data, in a transient model of focal cerebral ischaemia, showed that combining intravenous and subcutaneous administration of a CDK inhibitor, (S)-roscovitine, decreased significantly brain swelling and EB extravasation and was associated with neurological improvement. Further cellular analysis showed that (S)-roscovitine inhibited significantly endothelial activation, microglia proliferation and that it showed a trend toward decreased astrocytes proliferation and astrogliosis. PCA integrating preceding data allowed us to better understand the respective role of the NVU components and to suggest mechanisms associated with brain swelling, BBB disruption and cellular interactions.

We observed that (S)-roscovitine administered 90 min after ischaemia onset decreased strongly cerebral brain swelling by more than 50%. Very few studies reported a beneficial effect of non-pharmacological and pharmacological treatment on brain swelling after cerebral ischaemia (Shah and Kimberly, 2016).

We observed in the same animals that (S)-roscovitine treatment favoured neurological recovery unrelated to glucose level and body temperature (see Supplementary Table 1). Previous studies already showed neuroprotective and neurological recovery effect of (S)-roscovitine in rodent models of cerebral ischaemia (Menn *et al.*, 2010; Rousselet *et al.*, 2018) with a decrease of the size of infarction in treated animals. Both mechanisms of neuroprotection and anti-oedema effect may play a role in neurological recovery. Studies with the R enantiomer of roscovitine [For review, see Timsit and Menn (2012)] did not report anti-oedema effect on different models of focal ischaemia and may be related to a specific effect of the S form or the absence of oedema analysis. Other CDK inhibitor (Osuga *et al.*, 2000) studies also showed a

decrease of size of infarction in rodent model of focal ischaemia but did not mention anti-oedema effect.

A common rostro-caudal gradient was observed both on brain swelling and with EB suggesting that both events are linked. Furthermore (S)-roscovitine effect was mainly observed in the rostral cuts of the ischaemic brain. EB extravasation's roscovitine effect was supported by three different techniques: histofluorescence analysis based on the natural fluorescent property of EB (Saria and Lundberg, 1983), spectrophotometer analysis and EB macroscopic photonic analysis. To our knowledge, it is the first time that this EB fluorescence property is used to assess BBB permeability in a model of ischaemia. Rostro-caudal gradient does not appear to be frequently described and might be related to the severity of ischaemia which could be different in the rostral compared to the caudal part or to other unknown mechanisms (Choi *et al.*, 2009; Yli-Karjanmaa *et al.*, 2019).

This is the first observation, to our knowledge, concerning a CDK inhibitor beneficial effect on BBB permeability in ischaemia and other neurological diseases.

Cellular effect of (S)-roscovitine after focal ischaemia

Endothelial cells

The involvement of endothelial cells activation after brain ischaemia is no longer to be demonstrated (Pan *et al.*, 2016; Wong *et al.*, 2019). Here, we observed after focal ischaemia an increase of RECA-1 intensity, a cell surface antigen on rat endothelial cells (Duijvestijn *et al.*, 1992), in perilesional area and a greater increase in lesional area compared to healthy hemisphere. From this observation, we suggest that RECA-1 intensity may be related to endothelial activation after an endothelial stress associated with an increase of the protein level of RECA-1 protein, or even to endothelial oedema, and less likely at the acute stroke phase, a signal of neo-angiogenesis.

(S)-roscovitine decreased significantly RECA-1 immunofluorescence intensity in the perilesional cortex and tended to decrease not significantly in the perilesional DGN but not in the lesional area, i.e., the core of ischaemia. Differences in RECA-1 endothelial cells intensity between the lesion and the perilesional area may be explained by the severity of ischaemia while having a penumbra-like area in the perilesional areas. RECA-1 intensity has not been described in focal ischaemia. Furthermore, global analysis of occludin on western blot, a key specific protein at the tight junction between endothelial cells (Cummins, 2012), playing a role in BBB integrity, further supported the role of (S)-roscovitine in endothelial cells. It is not clear if (S)-roscovitine plays a role directly on endothelial cells or if this effect is related to an indirect effect on neurons, astrocytes or microglial cells. Studies in the CNS and outside support a direct role, at least partially, of (S)-roscovitine in endothelial

cells: (i) over-expression of CDK5 together with p35/p25 was observed in apoptotic brain endothelial cells in hypoxic regions of stroked tissue and was associated to cellular damages as responses to hypoxic condition (Mitsios *et al.*, 2007); (ii) (R)-roscovitine prevented endothelial activation and leukocyte-endothelial cell interaction *in vitro* and *in vivo*, in venules of mouse cremaster muscle, by inhibition of CDK5 and 9 (Berberich *et al.*, 2011).

To our knowledge, this is the first observation that a CDK inhibitor decreases RECA-1 activation and occludin depolymerization in ischaemic stroke. There are arguments (see above) supporting a direct effect of (S)-roscovitine on endothelial cells activation. Whether this effect predominates on arteries or veins remain to be determined.

Microglial inhibition by (S)-roscovitine

Resident microglia cells are activated from the first minutes of cerebral ischaemia. A proliferation peak of microglia is observed around 48–72 h post-stroke (Denes *et al.*, 2007). Microglia activation following stroke is predominantly harmful in the acute phase of ischaemic stroke (Thurgur and Pinteaux, 2019).

In our study, (S)-roscovitine treatment halved microglia number as observed by IB4 staining in the ischaemic hemisphere compared to vehicle. Although IB4 is a marker of both endothelial and microglial cells (Boscia *et al.*, 2013), morphologic-oriented counting allowed us to precisely evaluate microglia number. Another marker of microglia IBA1 confirmed our prior results. Inhibition of microglia proliferation by CDK inhibitor was also observed in a rat tMCAo model (Zhang *et al.*, 2009) with (R)-roscovitine but not (S)-roscovitine. Furthermore (R)-roscovitine was injected 24 h before MCA occlusion by intracerebroventricular infusion. Other publications also showed that (R)-roscovitine, decreased microglia activation or proliferation on other model of neurological injury (Hilton *et al.*, 2008; Kim *et al.*, 2019; Tomov *et al.*, 2019).

Here, we observed a major decrease of microglia's number with (S)-roscovitine administration after brain ischaemia as previously suggested but not shown (Timsit and Menn, 2012).

(S)-roscovitine's effect on reactive astrocyte

Reactive astrocytes, characterized by proliferation and astrogliosis [defined by GFAP upregulation (Zamanian *et al.*, 2012; Hol and Pekny, 2015)], promote infarct progression (Yao *et al.*, 2015), exacerbate inflammation (Colombo and Farina, 2016), compromise BBB function (Tan *et al.*, 2019) and aggravate cytotoxic oedema (Manley *et al.*, 2000; Liu and Chopp, 2016). No GFAP signal was detected in the lesion area itself probably because of astrocyte necrosis in the core of ischaemia. (S)-roscovitine decreased astrocyte's number as observed with

GFAP staining signal, after ischaemic stroke compared to vehicle in the DGN perilesional-boundary and showed a trend toward a smaller normalized GFAP intensity per astrocyte. Gutiérrez-Vargas *et al.* (2015) previously observed in tMCAO rat model that CDK5-RNAi intra-hippocampal injection was associated with a decrease in astrocyte hyperactivity (Gutiérrez-Vargas *et al.*, 2015). Becerra-Calixto *et al.* (2018), also observed that CDK5-KD astrocyte transplantation in a global cerebral ischaemia model prevented neuronal and astrocyte loss. Furthermore, (R)-roscovitine prevented astrogliosis and reactive astrogliosis in other acute and chronic experimental neurological models (Di Giovanni *et al.*, 2005; Hyun *et al.*, 2017; Zhong *et al.*, 2019).

Here, we observed an effect of (S)-roscovitine, possibly mediated by CDK5 inhibition, on reactive astrocytes.

Principal component analysis

From the idea that the activity of the brain is linked to local circulation (Roy and Sherrington, 1890) emerged the concept of NVU or neuro-glio-vascular unit which consists of an assembly of neurons, interneurons, astrocytes, microglia, basal lamina, smooth muscle cells, pericytes, endothelial cells and extracellular matrix (Hawkins and Davis, 2005). To decipher the complex relationship of some of these components, we analysed the quantitative variables of our study by PCA. To our knowledge, only few studies used PCA for quantitative cell-related biological phenomenon. Few reported on specific morphology of microglia (Fernández-Arjona *et al.*, 2017; Heindl *et al.*, 2018) and on the metabolic coupling of the human NVU (Maoz *et al.*, 2018). PCA of six histological variables, including neovascularization, oedema and neutrophil infiltration, was also used by Galiacy *et al.* (2011) to understand the relation between variables on the corneal scarring model. Furthermore, Ferguson *et al.*, (2013) crossed behavioural variables and histological variables to extract features that were conserved across different spinal cord injury models. However, we failed to identify studies integrating components of the NVU as variables for PCA, used here as an exploratory data analysis.

We conducted PCA on 16 animals for the seven correlated quantitative variables RECA-1, microglia number, EB, brain swelling, astrocytes number, astrogliosis, and finally stroke recovery as a supplementary variable. PCA differentiated treated from non-treated animals on dimension 1 with negative values in the treated animals, and positive values in the non-treated animals. Interestingly, stroke recovery presents a negative correlation with this dimension, while all other variables show a positive correlation. Dimensions 1 and 2 allowed the identification of two groups of co-varying variables: endothelial cells as identified by RECA-1 antibody, microglia number and EB with positive values on both dimensions, and astrocyte number, astrogliosis and brain swelling with negative values on dimension 2. This partition suggests different

mechanisms, one related to BBB in relation with endothelial cells integrity and microglia proliferation, and another one related to brain swelling and reactive astrocytes. Concerning the first supposed mechanism, endothelial cells obviously play a key role in BBB integrity, but PCA suggests that its integrity is dependent on microglia. It is consistent with actual knowledge that activated microglia can activate endothelial cells and induce endothelial necroptosis by triggering the production of cytokines or chemokines, reactive oxygen species and matrix metalloprotease (da Fonseca *et al.*, 2014; Chen *et al.*, 2019). Concerning the second supposed mechanism, covariance of brain swelling and reactive astrocyte, seen in the PCA and in the covariance matrix, interpretation seems more complex. Brain swelling that is measured in these experiments is generally attributed to vasogenic oedema; PCA analysis suggests that reactive astrocytes as studied by astrogliosis and astrocyte proliferation play a role in brain swelling. Whether this role is mediated by cytotoxic oedema prominent in astrocytes remains to be established (Stokum *et al.*, 2015). Interestingly, brain swelling was negatively correlated to stroke recovery. This is expected since swelling is an independent predictor of poor outcome after stroke (Battey *et al.*, 2014). These results therefore suggest that (S)-roscovitine effect is mediated by the modulation of the entire NVU response to ischaemia and not led by one single cell type. Correlation matrix confirms the strong relationship between NVU component including microglia, endothelial cells and astrocytes.

Conclusion

Here, we used a NVU integrated approach to understand the anti-oedematous effect of (S)-roscovitine. To our knowledge, this is the first observation, in ischaemic stroke, showing a CDK inhibitor beneficial effect on BBB permeability and brain swelling through endothelial-cells-activation inhibition and control of microglia and reactive astrocytes.

Supplementary material

Supplementary material is available at *Brain Communications* online.

Acknowledgements

The authors thank Dr Emmanuelle Génin (INSERM U1078, Université de Bretagne Occidentale) for helpful comments and review of statistical analysis. We thank the members of Animalerie Commune de l'UBO for assistance and supports in the experimental procedures.

Funding

Funding from Centre National de Recherche en Génomique Humaine of Commissariat à l'Énergie Atomique (CNRGH-CEA) was obtained to support Ozvan Bocher.

Competing interests

Serge Timsit is the co-inventor of a patent concerning (S)-roscovitine.

References

- Bach S, Knockaert M, Reinhardt J, Lozach O, Schmitt S, Baratte B, et al. Roscovitine targets, protein kinases and pyridoxal kinase. *J Biol Chem* 2005; 280: 31208–19.
- Battey TWK, Karki M, Singhal AB, Wu O, Sadaghiani S, Campbell BCV, et al. Brain edema predicts outcome after non-lacunar ischemic stroke. *Stroke J Cereb Circ* 2014; 45: 3643–8.
- Becerra-Calixto A, Posada-Duque R, Cardona-Gómez GP. Recovery of neurovascular unit integrity by CDK5-KD astrocyte transplantation in a global cerebral ischemia model. *Mol Neurobiol* 2018; 55: 8563–85.
- Berberich N, Uhl B, Joore J, Schmerwitz UK, Mayer BA, Reichel CA, et al. Roscovitine blocks leukocyte extravasation by inhibition of cyclin-dependent kinases 5 and 9. *Br J Pharmacol* 2011; 163: 1086–98.
- Berrousot J, Sterker M, Bettin S, Köster J, Schneider D. Mortality of space-occupying ('malignant') middle cerebral artery infarction under conservative intensive care. *Intensive Care Med* 1998; 24: 620–3.
- Boscia F, Esposito CL, Casamassa A, de Franciscis V, Annunziato L, Cerchia L. The isolectin IB4 binds RET receptor tyrosine kinase in microglia. *J Neurochem* 2013; 126: 428–36.
- Chen S-S, Tang C-H, Chie M-J, Tsai C-H, Fong Y-C, Lu Y-C, et al. Microglia-derived TNF- α mediates endothelial necroptosis aggravating blood brain-barrier disruption after ischemic stroke. *Cell Death Dis* 2019; 10: 31.
- Choi I-S, Kwon J, Kim Y-K. Neurological effects of Bojungikki-tang and Bojungikki-tang-gamibang on focal cerebral ischemia of the MCAO rats. *The Journal of Korean Oriental Medicine* 2009; 30: 53.
- Colombo E, Farina C. Astrocytes: key regulators of neuroinflammation. *Trends Immunol* 2016; 37: 608–20.
- Cummins PM. Occludin: one protein, many forms. *Mol Cell Biol* 2012; 32: 242–50.
- Denes A, Vidyasagar R, Feng J, Narvainen J, McColl BW, Kauppinen RA, et al. Proliferating resident microglia after focal cerebral ischemia in mice. *J Cereb Blood Flow Metab* 2007; 27: 1941–53.
- Di Giovanni S, Movsesyan V, Ahmed F, Cernak I, Schinelli S, Stoica B, et al. Cell cycle inhibition provides neuroprotection and reduces glial proliferation and scar formation after traumatic brain injury. *Proc Natl Acad Sci USA* 2005; 102: 8333–8.
- Duijvestijn AM, van Goor H, Klatter F, Majoer GD, van Bussel E, van Breda Vriesman PJ. Antibodies defining rat endothelial cells: RECA-1, a pan-endothelial cell-specific monoclonal antibody. *Lab Invest J Tech Methods Pathol* 1992; 66: 459–66.
- Ferguson AR, Irvine K-A, Gensel JC, Nielson JL, Lin A, Ly J, et al. Derivation of multivariate syndromic outcome metrics for consistent testing across multiple models of cervical spinal cord injury in rats. *PLoS One* 2013; 8: e59712.
- Fernández-Arjona MDM, Grondona JM, Granados-Durán P, Fernández-Llebrez P, López-Avalos MD. Microglia morphological categorization in a rat model of neuroinflammation by hierarchical

- cluster and principal components analysis. *Front Cell Neurosci* 2017; 11: 235.
- da Fonseca ACC, Matias D, Garcia C, Amaral R, Geraldo LH, Freitas C, et al. The impact of microglial activation on blood-brain barrier in brain diseases. *Front Cell Neurosci* 2014; 8: 1–13
- Frank JL. Large hemispheric infarction, deterioration, and intracranial pressure. *Neurology* 1995; 45: 1286–90.
- Galiacy SD, Fournié P, Massoudi D, Ancèle E, Quintyn J-C, Erraud A, et al. Matrix metalloproteinase 14 overexpression reduces corneal scarring. *Gene Ther* 2011; 18: 462–8.
- Gutiérrez-Vargas JA, Múnera A, Cardona-Gómez GP. CDK5 knock-down prevents hippocampal degeneration and cognitive dysfunction produced by cerebral ischemia. *J Cereb Blood Flow Metab* 2015; 35: 1937–49.
- Hacke W, Schwab S, Horn M, Spranger M, De Georgia M, von Kummer R. ‘Malignant’ middle cerebral artery territory infarction: clinical course and prognostic signs. *Arch Neurol* 1996; 53: 309–15.
- Hawkins BT, Davis TP. The blood-brain barrier/neurovascular unit in health and disease. *Pharmacol Rev* 2005; 57: 173–85.
- Heindl S, Gesierich B, Benakis C, Llovera G, Duering M, Liesz A. Automated morphological analysis of microglia after stroke. *Front Cell Neurosci* 2018; 12: 1–11.
- Hilton GD, Stoica BA, Byrnes KR, Faden AI. Roscovitine reduces neuronal loss, glial activation, and neurologic deficits after brain trauma. *J Cereb Blood Flow Metab* 2008; 28: 1845–59.
- Hofmeijer J, Kappelle LJ, Algra A, Amelink GJ, van Gijn J, van der Worp HB. Surgical decompression for space-occupying cerebral infarction (the Hemicraniectomy After Middle Cerebral Artery infarction with Life-threatening Edema Trial [HAMLET]): a multicentre, open, randomised trial. *Lancet Neurol* 2009; 8: 326–33.
- Hol EM, Pekny M. Glial fibrillary acidic protein (GFAP) and the astrocyte intermediate filament system in diseases of the central nervous system. *Curr Opin Cell Biol* 2015; 32: 121–30.
- Hyun H-W, Min S-J, Kim J-E. CDK5 inhibitors prevent astroglial apoptosis and reactive astrogliosis by regulating PKA and DRP1 phosphorylations in the rat hippocampus. *Neurosci Res* 2017; 119: 24–37.
- Jiang SX, Lertvorachon J, Hou ST, Konishi Y, Webster J, Mealing G, et al. Chlortetracycline and demeclocycline inhibit calpains and protect mouse neurons against glutamate toxicity and cerebral ischemia. *J Biol Chem* 2005; 280: 33811–8.
- Johnson CO, Nguyen M, Roth GA, Nichols E, Alam T, Abate D, et al. Global, regional, and national burden of stroke, 1990–2016: a systematic analysis for the Global Burden of Disease Study 2016. *Lancet Neurol* 2019; 18: 439–58.
- Kilkenny C, Browne WJ, Cuthill IC, Emerson M, Altman DG. Improving bioscience research reporting: the ARRIVE guidelines for reporting animal research. *PLoS Biol* 2010; 8: e1000412.
- Kim J-E, Park H, Choi S-H, Kong M-J, Kang T-C. Roscovitine attenuates microglia activation and monocyte infiltration via p38 MAPK inhibition in the rat frontoparietal cortex following status epilepticus. *Cells* 2019; 8: 746.
- Li BS, Sun MK, Zhang L, Takahashi S, Ma W, Vinade L, et al. Regulation of NMDA receptors by cyclin-dependent kinase-5. *Proc Natl Acad Sci USA* 2001; 98: 12742–7.
- Liu Z, Chopp M. Astrocytes, therapeutic targets for neuroprotection and neurorestoration in ischemic stroke. *Prog Neurobiol* 2016; 144: 103–20.
- Love S. Neuronal expression of cell cycle-related proteins after brain ischaemia in man. *Neurosci Lett* 2003; 353: 29–32.
- Lowry RN, Lewis Farr A, Randall RJ. Protein measurement with the folin phenol reagent. *J Biol Chem* 1951; 193: 265–75.
- Manley GT, Fujimura M, Ma T, Noshita N, Filiz F, Bollen AW, et al. Aquaporin-4 deletion in mice reduces brain edema after acute water intoxication and ischemic stroke. *Nat Med* 2000; 6: 159–63.
- Maoz BM, Herland A, FitzGerald EA, Grevesse T, Vidoudez C, Pacheco AR, et al. A linked organ-on-chip model of the human neurovascular unit reveals the metabolic coupling of endothelial and neuronal cells. *Nat Biotechnol* 2018; 36: 865–74.
- Meijer L, Borgne A, Mulner O, Chong JP, Blow JJ, Inagaki N, et al. Biochemical and cellular effects of roscovitine, a potent and selective inhibitor of the cyclin-dependent kinases cdc2, cdk2 and cdk5. *Eur J Biochem* 1997; 243: 527–36.
- Menn B, Bach S, Blevins TL, Campbell M, Meijer L, Timsit S. Delayed treatment with systemic (S)-roscovitine provides neuroprotection and inhibits in vivo CDK5 activity increase in animal stroke models. *PLoS One* 2010; 5: e12117.
- Meyer DA, Torres-Altoro MI, Tan Z, Tozzi A, Filippo MD, DiNapoli V, et al. Ischemic stroke injury is mediated by aberrant Cdk5. *J Neurosci* 2014; 34: 8259–67.
- Michinaga S, Koyama Y. Pathogenesis of brain edema and investigation into anti-edema drugs. *Int J Mol Sci* 2015; 16: 9949–75.
- Mitsios N, Pennucci R, Krupinski J, Sanfeliu C, Gaffney J, Kumar P, et al. Expression of cyclin-dependent kinase 5 mRNA and protein in the human brain following acute ischemic stroke. *Brain Pathol* 2007; 17: 11–23.
- Ohshima T, Gilmore EC, Longenecker G, Jacobowitz DM, Brady RO, Herrup K, et al. Migration defects of cdk5(-/-) neurons in the developing cerebellum is cell autonomous. *J Neurosci* 1999; 19: 6017–26.
- Osuga H, Osuga S, Wang F, Fetni R, Hogan MJ, Slack RS, et al. Cyclin-dependent kinases as a therapeutic target for stroke. *Proc Natl Acad Sci USA* 2000; 97: 10254–9.
- Pan Q, He C, Liu H, Liao X, Dai B, Chen Y, et al. Microvascular endothelial cells-derived microvesicles imply in ischemic stroke by modulating astrocyte and blood brain barrier function and cerebral blood flow. *Mol Brain* 2016; 9: 63.
- Rousselet E, Létondor A, Menn B, Courbebaisse Y, Quillé M-L, Timsit S. Sustained (S)-roscovitine delivery promotes neuroprotection associated with functional recovery and decrease in brain edema in a randomized blind focal cerebral ischemia study. *J Cereb Blood Flow Metab* 2018; 38: 1070–84.
- Roy CS, Sherrington CS. On the regulation of the blood-supply of the brain. *J Physiol* 1890; 11: 85–158.17.
- Sakai K, Tanaka Y, Tokushige K, Tanabe A, Kobayashi S. Basilar bifurcation aneurysms associated with persistent primitive hypoglossal artery. *Neurosurg Rev* 1998; 21: 290–4.
- Saria A, Lundberg JM. Evans blue fluorescence: quantitative and morphological evaluation of vascular permeability in animal tissues. *J Neurosci Methods* 1983; 8: 41–9.
- Shah S, Kimberly WT. The modern approach to treating brain swelling in the neuro ICU. *Semin Neurol* 2016; 36: 502–7.
- Shaw CM, Alvord EC, Berry RG. Swelling of the brain following ischemic infarction with arterial occlusion. *Arch Neurol* 1959; 1: 161–77.
- Shin BN, Kim DW, Kim IH, Park JH, Ahn JH, Kang IJ, et al. Down-regulation of cyclin-dependent kinase 5 attenuates p53-dependent apoptosis of hippocampal CA1 pyramidal neurons following transient cerebral ischemia. *Sci Rep* 2019; 9: 1–15.
- Stokum JA, Kurland DB, Gerzanich V, Simard JM. Mechanisms of astrocyte-mediated cerebral edema. *Neurochem Res* 2015; 40: 317–28.
- Tan S, Shan Y, Lin Y, Liao S, Zhang B, Zeng Q, et al. Neutralization of interleukin-9 ameliorates experimental stroke by repairing the blood-brain barrier via down-regulation of astrocyte-derived vascular endothelial growth factor-A. *FASEB J* 2019; 33: 4376–87.
- Thurgur H, Pinteaux E. Microglia in the neurovascular unit: blood-brain barrier-microglia interactions after central nervous system disorders. *Neuroscience* 2019; 405: 55–67.
- Timsit S, Menn B. Cyclin-dependent kinase inhibition with roscovitine: neuroprotection in acute ischemic stroke. *Clin Pharmacol Ther* 2012; 91: 327–32.
- Tomov N, Surchev L, Wiedenmann C, Döbrössy M, Nikkha G. Roscovitine, an experimental CDK5 inhibitor, causes delayed suppression of microglial, but not astroglial recruitment around intracerebral dopaminergic grafts. *Exp Neurol* 2019; 318: 135–44.

- Vahedi K, Hofmeijer J, Juettler E, Vicaut E, George B, Algra A, et al. Early decompressive surgery in malignant infarction of the middle cerebral artery: a pooled analysis of three randomised controlled trials. *Lancet Neurol* 2007; 6: 215–22.
- Wen Y, Yang S, Liu R, Simpkins JW. Cell-cycle regulators are involved in transient cerebral ischemia induced neuronal apoptosis in female rats. *FEBS Lett* 2005; 579: 4591–9.
- Wong R, Lénárt N, Hill L, Toms L, Coutts G, Martinez B, et al. Interleukin-1 mediates ischaemic brain injury via distinct actions on endothelial cells and cholinergic neurons. *Brain Behav Immun* 2019; 76: 126–38.
- Yao X, Derugin N, Manley GT, Verkman AS. Reduced brain edema and infarct volume in aquaporin-4 deficient mice after transient focal cerebral ischemia. *Neurosci Lett* 2015; 584: 368–72.
- Yli-Karjanmaa M, Clausen BH, Degn M, Novrup HG, Ellman DG, Toft-Jensen P, et al. Topical administration of a soluble TNF inhibitor reduces infarct volume after focal cerebral ischemia in mice. *Front Neurosci* 2019; 13: 1–18.
- Zamanian JL, Xu L, Foo LC, Nouri N, Zhou L, Giffard RG, et al. Genomic analysis of reactive astrogliosis. *J Neurosci* 2012; 32: 6391–410.
- Zhang Q, Chen C, Lü J, Xie M, Pan D, Luo X, et al. Cell cycle inhibition attenuates microglial proliferation and production of IL-1beta, MIP-1alpha, and NO after focal cerebral ischemia in the rat. *Glia* 2009; 57: 908–20.
- Zhong Y, Chen J, Chen J, Chen Y, Li L, Xie Y. Crosstalk between Cdk5/p35 and ERK1/2 signalling mediates spinal astrocyte activity via the PPAR γ pathway in a rat model of chronic constriction injury. *J Neurochem* 2019; 151: 166–84.